Chapter 2

Literature Review: CVD Risk Biomarkers Measurement and Quantification

2.1 Historical Background

Understanding the atherosclerosis progression and plaque deposition lays the foundation of the increasing CVD risk. The CVD risk is enhanced by the vulnerable plaque components present inside the LI and MA region. Researchers proposed some CVD risk biomarkers such as cIMT, plaque area, and lumen diameter which are used by the medical practitioners. Further, various ML and DL based techniques have been used in past to automatically measure these biomarkers.

The current chapter highlights the importance of carotid biomarkers in CVD risk assessment, and their measurement by modern DL techniques. Previous studies have explored the DL techniques in CVD risk assessment, but they are not focused on biomarkers of all segments of carotid artery. Current review focuses on PA of CCA and ICA, and cIMT measurement. Also, we reviewed plaque tissue characterization and classification into its components. Since, ICA plaque area is large and unevenly distributed, therefore IMT measurement at ICA location is not performed by the radiologists. We have also compared current DL techniques against previous ML based techniques. Lastly, all risk factors with significant impact on CVD are also studied. Thus the review provide a complete overview of the CVD risk from generation and progression of the atherosclerosis disease, vital biomarkers, and their measurement using ML and DL techniques.

2.2 Generations of Segmentation Methods

2.2.1 Machine Learning based Methods of CVD Detection

Since there are few radiologists compared with the significant number of medical images generated daily, manual screening is slow and error-prone. Therefore, a computer-aided diagnosis (CAD) system or decision support system (DSS) is needed to overcome these drawbacks of manual measurements. Machine learning (ML) has proved to be an excellent tool for learning from experiences automatically. The polyline distance metric method is a benchmark for segmentation and used in many studies [31, 73-76] for region-of-interest (ROI) detection. Biswas *et al.* used this method in combination with convolution neural networks (CNNs) to detect LD automatically [77].

The shape-based approach developed by Cootes *et al.* [78] inspired researchers to develop methods for LD and cIMT measurements [79-82]. ML tools for measuring plaques and stenosis rely upon accessing the texture from the ROI. These texture features contain spatial and temporal information about the images' ROI. Depending on system design and analysis, the extracted features may indicate statistically significant alterations, which sometimes enhance the accuracy and reliability of the system and sometimes collapses the estimations. ML-based risk assessment systems using LD and cIMT as biomarkers overcome the difficulties of manual methods [36, 37, 83, 84]. In this regard, Saba *et al.* and Araki *et al.* show that the careful extraction and selection of features is an essential step for ML systems. Detailed investigation of the ML system designed by Araki *et al.* [37, 83, 84] and Saba *et al.* in [36] reveals various checkpoints, e.g., ROI detection, feature extraction, and feature selection, that can improve image classification and evaluation and, therefore, the overall performance of the system [37, 83, 84].

2.2.2 Deep Learning Based Method for CVD Detection

Deep-learning-based techniques, such as CNN's, overcome these checkpoints and improve the system's ability, hence becoming a very attractive tool for the analysis of medical images. These brain-inspired deep neural networks use convolutional, pooling, and fully connected layers to extract features from images, and the depth of the network provides highly improved feature maps. However, CNN layers use a large stack of images; therefore, the depth of the network increases the computational costs; hence, computations performed on standard central processing units (CPUs) may slow down the whole operation. Modern graphic processing units (GPUs) are built to process a large amount of data in parallel and do not affect the speed of the CPUs; therefore, these units can speed up the operation and measure in almost real-time [77, 85, 86].

The Deep-learning (DL) systems designed by the Biswas *et al.* in [87] which used encoder and decoder layers; the system created by Sudha *et al.* [88] based on a 10-layer CNN; and the autoencoders used by Menchón-Lara *et al.* [89] have gained remarkable success in cIMT measurements compared to conventional ML methods. Biswas *et al.* [87] showed an improvement of 20% in measuring cIMT values compared to sonographers using a two-stage system (a class of AtheroEdge™ system). Furthermore, with their DL system consisting of 13 encoder layers and three upsample decoder layers, Biswas *et al.* [77] have significantly improved lumen characterization based on US images. Zreik *et al.* [86] carried out a similar approach to identify coronary plaques and stenosis in coronary CT angiographic images.

2.3 Deep Learning in other Medical Imaging Applications

Apart from making contributions to implementing DL systems, many researchers have attempted to write reviews on DL in medical imaging. In their studies, Tandel *et al.* [90] wrote about brain cancer classification, Liu *et al.* [91] focused on medical ultrasound, and Lundervold *et al.* [92] concentrated on MRI images. Saba *et al.* [93] and Meyer *et al.* [94] discussed different aspects of the DL strategy in radiology. Nillmani *et al.* developed a deep learning based system for multiclass classification of the lung images affected from bacterial pneumonia, covid-19, and tuberculosis [95]. Based on the above studies, we can write an informative review of varying segmentation techniques using ML and DL systems in vascular imaging. Further, in this review, we focused on automated detection of LD, cIMT, and the bulb in US images, using various ML and DL techniques. We also addressed techniques that are an amalgamation of conventional and DL methods. Table 2.1 lists some of the studies involving deep learning applications in medical images.

2.4 UNet Based Segmentation Model and Its Variants

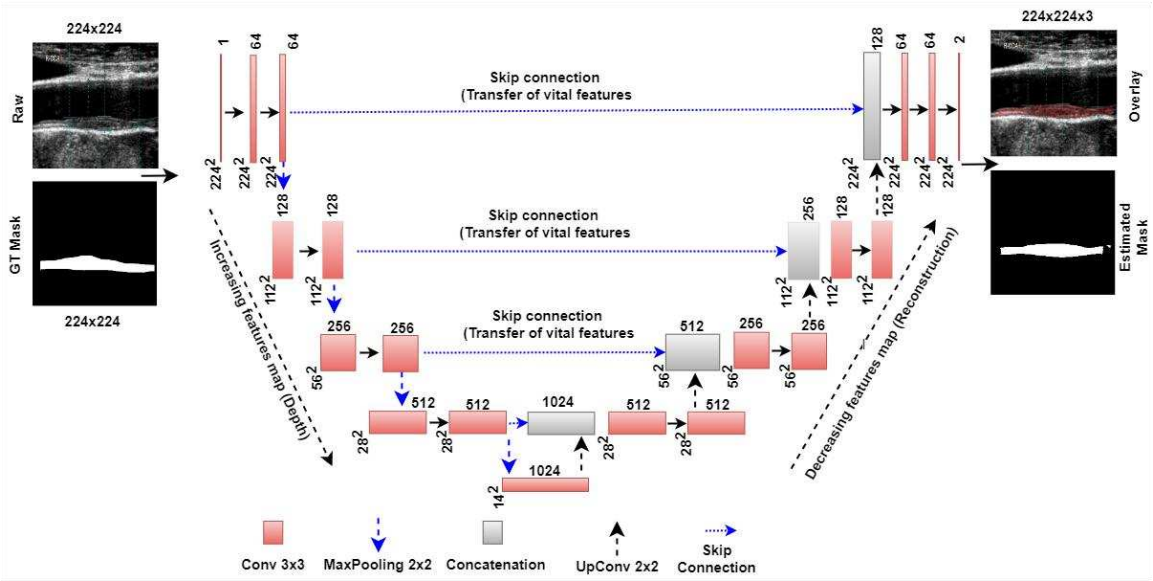

Figure 2.1 Basic UNet architecture for carotid plaque segmentation.

In the recent years UNet based deep learning model has been proven successful in medical image segmentation. Figure 2.1 shows four stage encoder-decoder architecture for medical image segmentation. Some researchers have used basic UNet model for carotid plaque segmentation [68, 71, 72, 96]. However, many researchers have proposed variations in encoder and decoder stages, or skip connections and sometimes amalgamation of two solo deep learning models to form a HDL model. Such an effort was first made by Jain *et al.* [97] by combining two SDLs UNet and SegNet to form SegNet-UNet HDL. The resultant HDL model has feature extraction capability of both models. In the same work the skip

connections of UNet were replaced by intermediate feature extraction blocks. These intermediate blocks are connected to previous layer only with the same feature map dimensions. This architecture is described by them as UNet+ architecture, and has better spatial feature extraction from encoder stages. Further, authors used combination of UNet+ and SegNet to form a SegNet-UNet+ HDL architecture, which again has feature extraction capability of both models.

Another variation of UNet is presented for carotid plaque segmentation by Zhou *et al.* [98] as UNet++. It is extension of UNet+ model by connecting all intermediate layers to all previous stages of the same feature map dimension. Their model has been used for CCA and ICA plaque segmentation and has some promising segmentation results.

The same UNet++ model has been recently used in a study by Jain *et al.* [99] for carotid plaque segmentation using a series of 'U-shaped' architectures. They proposed a series of new HDL architectures such as Inception-UNet, Squeeze-UNet, and Fractal-UNet for carotid plaque segmentation. These models have some unique advantages such as low memory, low training parameters, and low training time. A seven time reduction in model size could be seen in their Squeeze-UNet and Fractal-UNet models which can be used for web based, and cloud based applications. Further, they compare their HDL models against some of the previous SDL models such as UNet, UNet+, UNet++, and UNet3P (UNet+++). The SDL and HDL models' comparison show almost equal performance with some advantages of HDL models mentioned above. UNet3P is another unique SDL architecture they demonstrated in their study for carotid plaque segmentation. Unlike UNet++, UNet3P has addition of features at decoder stages from all encoder stages. Thus UNet3P architecture gets the advantages of adding multiscale features from different encoder stages to a decoder stage. Lastly, they validated their studies against Autoencoder based architecture. An autoencoder can be described as a UNet without skip connections. Thus, no spatial features are transferred from encoder to decoder without skip connections and autoencoder loses its significance in carotid plaque segmentation.

Meshram *et al.* [100] incorporated dilation in the convolution layers of the basic UNet models to enhance its performance in plaque segmentation. Carotid and coronary plaques are developed by the same atherosclerosis disease and have high correlation [83, 84]. Therefore any model developed for coronary interventions can be used for carotid arteries as well. Keeping this in mind we included in our review a dual-path UNet model developed by Yang *et al.* [101] for coronary artery wall segmentation in intravascular ultrasound (IVUS) images of coronary arteries.

Table 2.1 Deep learning UNet models for Biomedical Image Segmentation.

Authors	Image type	DL Technique	Metrics	Findings
Wei *et al.* [102]	Retinal vessel segmentation (OCT)	Genetic UNet	F1= 0.8314, ROC=0.9885	Trainable parameters-0.27M against 31.03 for UNet
Mar Villa *et al.* [70]	CCA, Bulb	DenseNets	PA, cIMT	Mean cIMT error = 0.022 (CCA) =0.06 (Bulb)
Zhang *et al.* [103]	Lungs CT	Dense-Inception UNet	DSC, JI, ACC, AUC	DSC= 0.9892, JI= 0.9871 ACC=0.9935, AUC=0.9903
	Retina Blood vessel (OCT)	Dense-Inception UNet		DSC= 0.9582, JI= 0.9338 ACC=0.9657, AUC=0.9802
	Brain Tumor MRI	Dense-Inception UNet		DSC= 0.9892, JI= 0.9940 ACC=0.9970, AUC=0.9867
Punn *et al.* [104]	Nuclei microscopy image	Inception-UNet	IoU, ACC	IoU=0.6523, ACC=0.9745
Park *et al.* [105]	Murine carotid artery ultrasound	IUNet: DL-based US imaging for flow–vessel dynamics (DL-UFV)	DSC	0.94(synthetic images) 0.90(in vivo test images)
Balaha *et al.* [106]	Lung X-ray images			
Biswas *et al.* [87]	CCA Ultrasound	Multiresolution(Phase1) CNN(Phase2) ML(Phase3)	GT vs AtheroEdge	LI Error 0.077±0.057 mm MA Error 0.113±0.105 mm cIMT Error 0.126±0.134 mm

Table 2.2 CCA and ICA Plaque segmentation Deep learning techniques.

Authors	Patients/Images	DL Methods	Metrics	Outcome	Area To address[#]
Cuadrado-Godia *et al.* [43]	P = 204; N= 396	3 stage DL system (Encoder:VGG16; Decoder:FCN)	gTPA = 20.52 mm^2 19.44 mm^2 DL1; DL2	CC: gTPA and cIMT = 0.92 (DL1); = 0.94 (DL2)	1, 2,3,6
Biswas *et al.* [107]	N = 250	Customized DL model for stage 1 (Characterization) and 2 (Segmentation)	PA error 2:7939 ±2:3702 mm^2	CC: 0.89 ($p<0.0001$	1,2, 4,6
Zhou *et al.* [98]	N_1 = 144; N_2 = 510	UNet++	ΔTPA= -0.44±4.05 mm^2	CC: AI vs GT ($r=0.972$, $p<0.001$) DSC = 85.7%	1,2,5
Zhou *et al.* [71]	N_1 = 144; N_2 = 510	Modified UNet	ΔTPA =0.05±7.13 mm2 ; 0.8±8.7 mm2	Time = 8.3 ±3.1 ms	2,3,4,5,6

Zhou *et al.* [108]	N=56	Carotid-Net	DSC = 80.34±7.94	HD = 11.44±6.20 mm MSD = 1.63±1.38 mm	2,3,4,5,6
Ma *et al.* [109]	P=333; N=1332	VGG16; FP-VGG16; OSFP-Net	ACC: 86.6%; 93.9%; 97.3%;	F1 Score 79.8 ± 5.4 91.2 ± 4.7; 95.9 ± 2.8;	1,2,3,4,5,6
Jain *et al.* [110]	N_1=330; N_2 = 300	UNet (Testing on unknown dataset)	Tr=(N_1+N_2)*0.9 Te =(N_1+N_2)*0.1 ACC:99.01; DSC:86.89; CC:0.92; (Testing on known dataset)	Tr:N_1;Te:N_2 ACC:98.55; DSC:78.38; CC:0.80; Tr:N_2;Te:N_1 ACC: 98.67; DSC:82.49; CC: 0.87	2,4,5
Liapi *et al.* [68]	P=201; N1=150,N2=30;N3=15	UNet	DSC: 0.736±0.10 JI: 0.583±0.12	KI:0.728±0.10 HD:0.65±0.19	2,4,5,6
Meshram *et al.* [100]	P= 101; N=352	UNet, Dilated-UNet, Semi-UNet, Semi-Dilated-UNet	U-Net 0.48± 0.24; Dilated-U-Net 0.55± 0.19; Semi-U-Net 0.83± 0.05; Semi-dilated U-Net 0.84± 0.05;	Hausdroff Error U-Net 1.71 0.38 Dilated U-Net 1.60	2,5,6

P= Number of patients; N= Number of Images; KI=Cohen's Kappa Coefficient; HD=Hausdorff Distance; MSD = Mean Square Distance

Area To address[#]

1-Reduce the complexity of the system

2- Improve the model performance

3- Benchmark with other model

4- Improvement in the DL architecture

5- Reduce training time

6- Benchmarking with other databases

Above discussed models till their development, proved to be the best for carotid plaque segmentation in ultrasound images. However, most of the studies were performed on databases from a single centre or same ethnic group, therefore the same model when applied for other databases are lacking in performance. This means the DL based systems have bias in their design, which is discussed in detail in later section of this chapter. Thus, an attention based mechanism can be applied to enhance feature extraction capability of the UNet model. Keeping this idea in mind Jain *et al.* deployed an attention based mechanism in UNet based model for plaque segmentation in an unseen database. While the previous models lack in performance on unknown database, the attention-UNet is giving good segmentation results. Thus, in our view the attention mechanism can be applied to other UNet models as well, to explore their added ability of attention-mechanism.

2.5 Critical Remarks: Quantitative Assessment of Carotid Biomarker using Deep Learning

Various deep learning architectures have been proposed by the researchers in the past few years for carotid artery plaque segmentation. Some architecture was focused upon CCA section, ICA section or both, or bulb area while development.

2.5.1 CCA Plaque area segmentation

Most of the architectures found in the literatures focused upon CCA plaque area segmentation. As discussed earlier CCA sections are easy to capture and therefore diagnosed by many sonographers. Many research groups have put effort on CCA plaque segmentation and classification. Earlier strategies belong to machine learning techniques, however recently they developed DL strategies for the same. Table 2.2 lists some of the previous studies in CCA plaque segmentation. In year 2018 Cuadrado-Godia *et al.* developed a three stage DL system to measure found cIMT and gTPA simultaneously from CCA US image [43]. They used a VGG16 network as an encoder and FCN as decoder stages. Their DL system found a good correlation between cIMT and gTPA (CC = 0.92 DL1; CC=0.94 DL2).

Recently, UNet based supervised learning techniques are proved best for medical image segmentation. Also, variation of basic UNet models are being utilized for various medical imaging tasks such as brain tumours, covid-19 affected lung segmentation, pelvic area organs, CCA and ICA plaque. Recently, Jain *et al.* developed some hybrid deep learning models such as SegNet-UNet to segment the moderate carotid plaque area from CCA images [96]. The hybrid deep learning model showed equal performance compared to solo DL model UNet but had a smaller size and faster operations. In another approach, Biswas *et al.* used a two-stage model and a patch (carotid image patches) based approach to characterize and segment the plaque area [107]. They didn't use the same UNet type of model, but their model incorporates encoder and decoder modules in the segmentation stage with only one skip connection. The correlation coefficient between AI estimated and GT area is 0.89 and the plaque area error was 2.7939±2.3702 mm^2.

Zhou *et al.* proposed a variation of UNet model with dense skip connections, i.e. UNet++ for medical image segmentation [111]. The proposed model proved useful for MRI, CT, histopathology, and electron microscopy (EM) image segmentation. Another group of researchers from China, Zhou *et al.* deployed UNet++ model for CCA and ICA plaque segmentation [98]. They tested the model on two datasets from Canada (Stroke Prevention and Atherosclerosis Research Centre: SPARC) and Wuhan, China. The SPARC dataset consists of 144 patients, and the China dataset consists of 497 patients. Both datasets contains plaque images of CCA and ICA sections. Best mean total plaque area difference for CCA images are 2.91±1.97 mm^2 and 5.55±4.34 mm^2 for ICA images. Same team of authors used similar datasets for plaque area measurement using modified UNet models [71]. TPA differences between AI estimated and GT plaque area for models 1 and 2 are 0.05±7.13 mm^2 and 0.8±8.7 $mm^{2,}$ respectively. The basic UNet model finds another application in carotid artery segmentation from large volumes of images from CTA by Zhou *et al.* [108]. Recently, Ma *et al.* proposed a four path object specific network to segment the plaque from transverse and longitudinal section of the carotid artery [109]. All plaque area measurement models suffered from cohort knowledge while training and testing the system.

Zhang *et al.* addressed the issue of generalization of DL based system in medical imaging due to domain shift from one hospital to another, different machine version/model, patient cohort, and imaging methods [112]. Keeping all issues in view, Jain *et al.* in an article used some hybrid and solo DL models for unseen data experiments [110]. In this strategy the hybrid DL models were deployed for multicity, multi-ethnic, and multi-device database. This means model trained with one type of database was tested on second type of database and vice-versa. Many researchers have used UNet and its variation for carotid plaque segmentation. Meshram *et al.* proposed three more variations of UNet, dilated-UNet, semi-UNet, and dilated-semi-UNet for CCA plaque segmentation [100]. Figure 2.2 shows some examples of CCA plaque segmentation in Hong Kong and Japanese database images.

2.5.2 ICA Plaque area Segmentation

Recently, Jain *et al.* developed some hybrid DL models such as SegNet-UNet and SegNet-UNet+ by combining some solo models such as UNet, and UNet+ with SegNet. Each model was developed and compared with two loss function cross-entropy and dice similarity coefficient [97]. In both hybrid and solo DL models, CE-loss function proved to be the best choice for plaque segmentation. Figure 2.3 shows GT-plaque and estimated plaque (red) and their absolute difference (in green) in moderate and high risk ICA images.

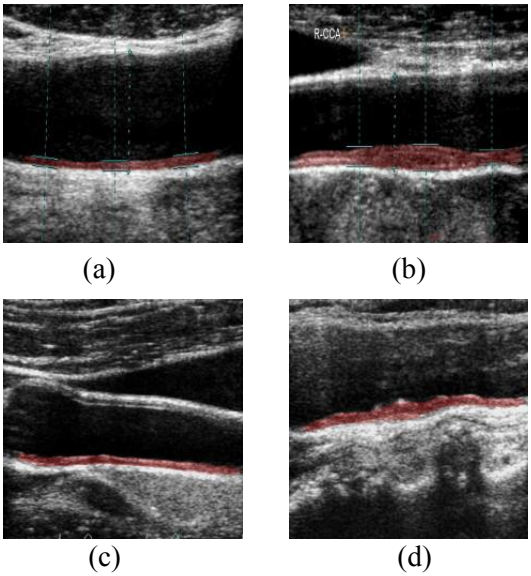

Figure 2.2 CCA Plaque area measurement in Japanese diabetic patients database (a) low (b) moderate risk and Hongkong database (c) low (d) moderate risk.

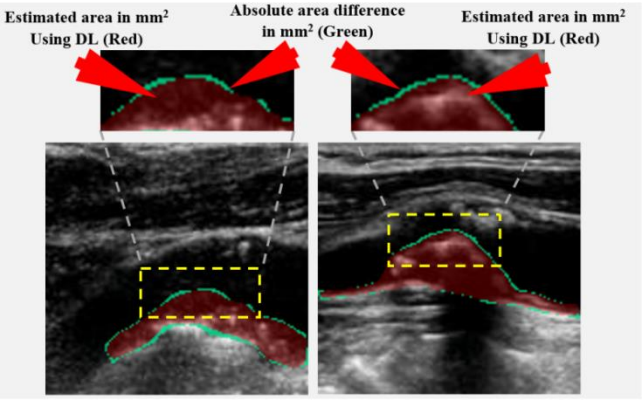

Figure 2.3 ICA Plaque segmentation from moderate risk and high-risk patients' US image.

2.5.3 CCA IMT measurement

Aside from carotid plaque segmentation, intima-media thickness and lumen diameter are also important leading biomarkers for diagnosing stroke risk. cIMT is a widely used clinical parameter for stroke risk assessment. Researchers have proved its clinical significance in research [36, 39]. After many clinical trials and studies, clinicians and researchers found a benchmark thickness value of 0.9 mm that could be used for risk stratification. Table 2.3 lists some of the benchmark studies in cIMT measurement. Biswas *et al.* proposed a three-phase model for cIMT measurement. The first phase used the multiresolution technique for lumen (LR) or inter-adventitial region (IAR) identification [87]. The second phase is an encoder-decoder-based DL model which is mainly designed for semantic segmentation of the plaque area.

Table 2.3 cIMT segmentation Deep learning techniques.

Authors	Cuadrado-Godia *et al.* [43]	Biswas *et al.* [107]	Zhou *et al.* [116]	Meiburger *et al.* [115]	Laxmi prabha *et al.* [114]	Zhou *et al.* [113]	Biswas *et al.* [87]	del Mar Vila *et al.* [70]
Patients/Images	P = 204; N= 396	N=250;	P=11; N=4070;	N=500	P = 110 (55 Normal, 55 Diabetic) 1809 Images	P=38, N=152 (3DUS)	N=396	N = 8000 (CCA, Bulb)
DL techniques	3 stage DL system (Encoder: VGG16; Decoder:FCN)	Two stage DL model for (custom nodel)	AlexNet	UNet	VGG16	CNN, UNet	Two stage DL system DL1 and DL2 (Encoder Decoder based)	DenseNet
Metrics	cIMT=0.91 mm; 0.88 mm DL1;DL2 CC: gTPA and cIMT = 0.92 (DL1); = 0.94 (DL2)	ΔcIMT = 0:0935 ±0:0637 mm CC: 0.99 (p < 0.0001),	Reduced annotation cost by 81%	ΔcIMT: 106±89 µm (absolute) 160±140 µm (intraobserver bias)	AUC: 0.602 (0.497–0.707, p < 0.05); 0.809 (95% CI; 0.721–0.897, p < 0.05); 0.806 (95% CI; 0.722–0.891, p < 0.05); 0.813(95% CI; 0.732–0.893, p < 0.05).	DSC of 96.46 ± 2.22% (MAB)	ΔcIMT = 0.126±0.134 mm (DL1) 0.124±0.100mm (DL2)	CC=0.81, mean Δ = 0.02 mm CCA mean Δ = 0.06 mm Bulb

MAB = Media Adventitia Boundary;

Further, in phase three segmented area is converted into LI/MA boundaries to calculate cIMT. Again, Biswas *et al.* presented a two-stage DL model for the characterization and segmentation of cIMT from CCA moderate plaque images [107]. In the first stage, they characterized or localized the region of interest, i.e. plaque wall; in the next stage, they segmented the plaque boundary and cIMT. Both of their

work presented a multiphase system for cIMT segmentation. Figure 2.4 shows LI and MA borders and cIMT measurement in high-risk and low risk CCA images.

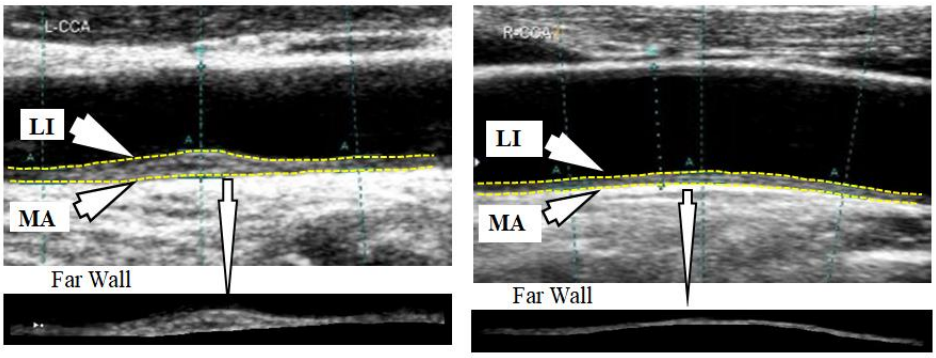

Figure 2.4 cIMT segmentation in high-risk (left) and low-risk (right) CCA US images.

2.5.4 Plaque Tissue Characterization

Plaque tissue characterization into symptomatic and asymptomatic categories is also challenging in carotid imaging. Taking up this challenge Saba *et al.* proposed six deep learning-based models for the classification of asymptomatic and symptomatic plaque [117]. Their system utilized multi-centre database from two cities therefore is free from data selection bias. Visual observation and semi-automated methods are often proved wrong or less efficient tissue characterization. Skandha *et al.* proposed various hybrid DL models for symptomatic and asymptomatic tissue characterization from carotid plaque patches [118]. Lekadir *et al.* [119] were the first to propose a CNN-based method for automated characterization of plaque composition in carotid ultrasound. The plaque components lipid, fibrous, and calcified tissue were successfully segmented from the plaque patches. Khanna *et al.* reviewed the plaque phenotype and cardiovascular risk assessment using ML and DL techniques [120]. Boi *et al.* studied coronary atherosclerotic plaque tissue characterization in intravascular OCT images [121]. Figure 2.5 shows symptomatic and asymptomatic classification of carotid plaque tissue using deep learning methods.

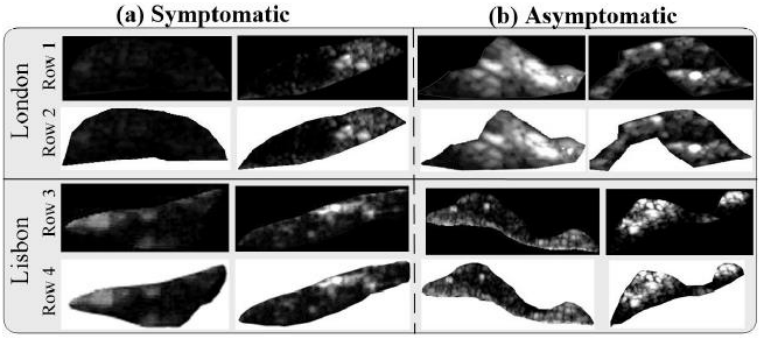

Figure 2.5 Plaque classification into symptomatic and asymptomatic categories. (With permission from Saba *et al.* [117])

2.6 Hardware and software for DL system

One of the most important reasons for the development of DL systems in medical image segmentation is the widespread availability of open-source software packages. Some of these open-source ML frameworks include Tensorflow, Theano, PyTorch, CUDNN, and Caffe. Another contribution to the development of DL systems is the availability of GPU and GPU core-computing libraries. GPUs have a considerable number of smaller cores compared to a general-purpose CPU, as shown in Figure 2.6. CUDA (Compute Unified Device Architecture) or OpenGL facilitates these GPUs with a large number of cores for accessing parallel computing. CUDA provides a parallel computing platform through an application programming interface (API) developed by NVIDIA™ for GPUs. All the above-mentioned GPU frameworks and GPU computing libraries are nowadays supported by Python, MATLAB, and C++.

2.7 Biases in Deep learning Based Systems

Deep learning based CVD risk assessment system uses clinical data such as US, MRI, CT, and PET images from hospitals and research centres. The DL based DSS systems have shown promising results. However, many of the reported studies use only one segment of the artery such as ICA, CCA or bulb. Further, the acquisition of database was done at one centre or from same models of equipment. Moreover, patients are from same ethnic background or having specific disease cohort. In some studies images are annotated by a single radiologists or researcher and not verified by other researchers due to unavailability of the manpower. Lastly, some researchers used only one or two DL models for classification and segmentation purpose, however they didn't compare their models against some validated experiments. Thus, we can conclude that the AI based system is biased towards data selection, model selection, data source, no validation by other model, race, and variability analysis. Many other types of biases also exists which are not discussed here, but they affect the clinical results. Thus, these biases must be discussed in details while designing the DSS systems.

2.8 Conclusions

In this chapter, we have reviewed the applications of DL technology in the field of CVD risk assessment. In the past few years, DL has emerged as a free and extensive technology in the field of AI. Many researchers have deployed DL strategies for CVD biomarker measurement. Further, we have focused our study on cIMT, PA, and LD measurement in the CCA and ICA US images. Previously, researchers have focused mainly on the CCA and applied ML and DL strategies to CCA biomarker measurement. Although a few researchers have shifted their attention to PA measurements of ICA images, such studies are still in the minority. Further, clinically validated and scientifically approved methods that are accepted by medical experts are still needed.